Caetano-Pinto et al.:

Amplifying the Impact of Kidney Microphysiological Systems: Predicting Renal Clearance Using Mechanistic Modelling Based on Reconstructed Drug Secretion

Supplementary Data

Table of Contents

1 Primary human renal proximal tubule epithelial cells (RPTEC)

Tab. S1: Supplier specifications of the RPTEC and kidney tissue used

RPTEC				
Supplier	Biopredic (https://www.biopredic.com/)			
Batch	RPT101029			
Donor gender	Female			
Donor age	50 years			
Specimen collection	Renal outer cortex nephrectomy			
Cell isolation	Percoll density-gradient centrifugation			
Storage	Cell culture medium containing 10% DMSO			
Quality control (supplier)	TEER measurements (170 Ω/cm^2) and rhodamine efflux			
Renal cortex samples				
Sample	Supplier	Donor sex	Age	Procedure
#1	BioIVT	79	Female	Nephrectomy
#2	BioIVT	68	Male	Nephrectomy
#3	Sahlgrenska Hospital	65	Female	Nephrectomy

doi:10.14573/altex.2204011s

2 Antibodies, specificity evaluation and localization

Tab. S2: Antibodies used for immunofluorescence

Primary antibody	Reference	Species	Dilutions	
			2D-plastic	Kidney-MPS
ZO1	610966/BD	mouse	1:500	1:200
OCT2	HPA008567/Sigma	rabbit	1:500	1:200
P-gp	ab170904/Abcam	rabbit	1:500	1:200
Na^+K^+-ATPase	ab196884/Abcam	rabbit	1:100	1:100
Acetylated tubulin	T12-11/Sigma	mouse	1:500	1:200
OAT1	AB131087/Abcam	rabbit	1:500	1:100
Secondary antibody[a]				
Alexa Fluor 555 anti-mouse	A21424	goat	1:500	1:100
Alexa Fluor 555 anti-rabbit	A21429	goat	1:500	1:100

[a] Secondary antibodies were co-incubated with Phalloidin-488 (anti-F-actin; 1:200) and Hoechst 33342 (50 mM; 1:1000).

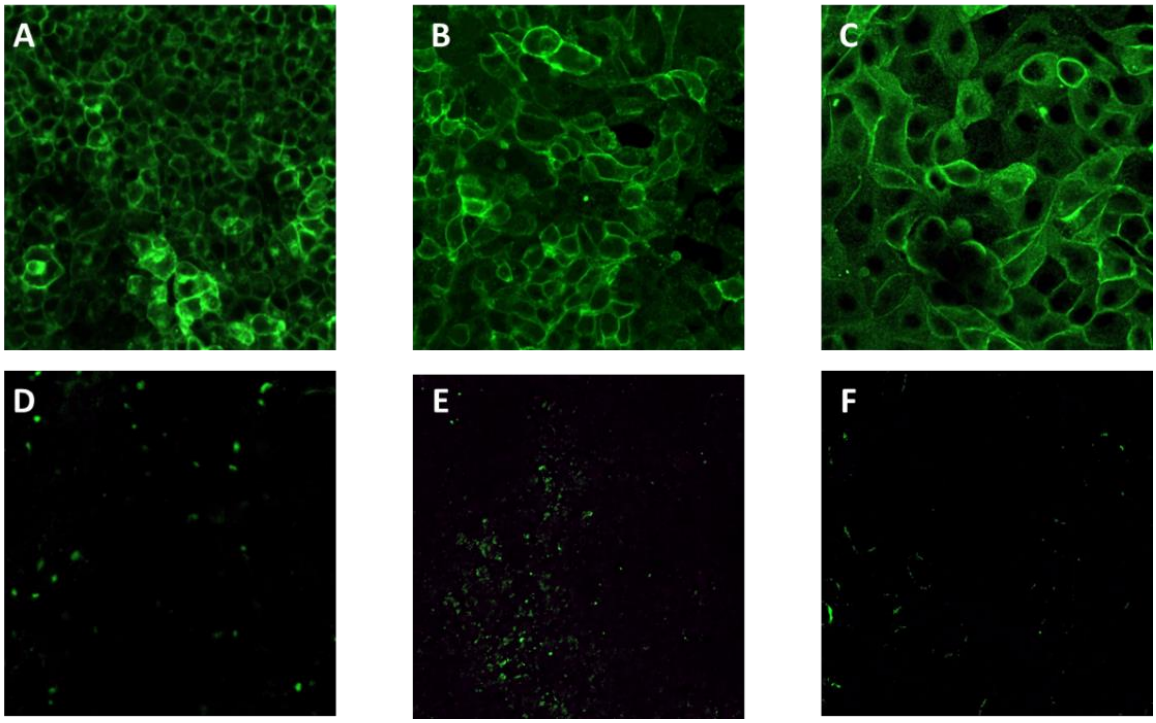

Fig. S1: Specificity of drug transporter antibodies evaluated in overexpression cell lines
Commercially available antibodies against membrane drug transporters are often reported as lacking specificity for their intended targets. To confirm that the antibodies used in this study recognize the drug transporters analyzed, immunostainings were performed in cell lines overexpressing OCT2 (HEK), OAT1 (HEK) or P-gp (MDCK). HEK-OCT2 (A) and HEK-mock transfected cells (D) were used to test the OCT2 antibody (dil. 1:500). HEK-OAT1 FlpIn (B) and HEK-FlpIn mock transfected cells (Zou et al., 2018) (E) were used to test the OAT1 antibody (dil. 1:500). MDCK-P-gp (C) and MDCK wild type cells (F) were used to test the P-gp antibody (dil. 1:1000). Secondary antibodies were used diluted 1:500 in combination with Hoechst 33342 1:1000.

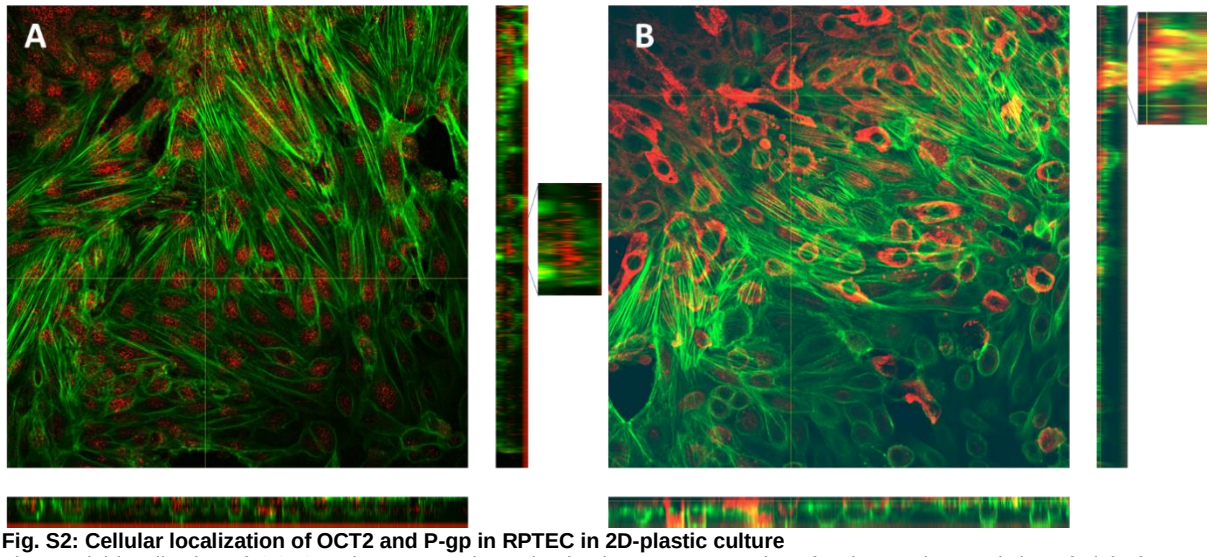

Fig. S2: Cellular localization of OCT2 and P-gp in RPTEC in 2D-plastic culture
The spatial localization of OCT2 and P-gp was determined using reconstructed confocal Z-stacks consisting of eight frames each (2 µm apart) after staining for f-actin (Phalloidin 488: green) and OCT2 or P-gp (Alexa555: red). F-actin is seen delineating the cell boundaries in the orthogonal views. OCT2 is mostly localized intracellularly and does not colocalize with the membrane (A). P-gp is expressed both intracellularly and in the membrane, evident from the yellow stain that results from f-actin and P-gp co-localization (B).

3 Gene reference list, statistics and housekeeping genes

Tab. S3: List of renal proximal tubule genes analyzed

Gene symbol [Protein name]	Hs-code (Thermo Fisher)	Gene name
AQP1	Hs01028916_m1	aquaporin 1 (Colton blood group)
CUBN	Hs00153607_m1	cubilin
HNF4A	Hs00230853_m1	hepatocyte nuclear factor 4 alpha
GGT1	Hs00980756_m1	gamma-glutamyltransferase 1
HPRT1	Hs02800695_m1	hypoxanthine phosphoribosyltransferase 1
LRP2 [Megalin]	Hs00189742_m1	LDL receptor related protein 2
ABCC4 [MRP4]	Hs00988721_m1	ATP binding cassette subfamily C member 4
ABCB1 [P-gp]	Hs00184500_m1	ATP binding cassette subfamily B member 1
SLC22A2 [OCT2]	Hs01010726_m1	solute carrier family 22 member 2
SLC22A6 [OAT1]	Hs00537914_m1	solute carrier family 22 member 6
SLC22A8 [OAT3]	Hs00188599_m1	solute carrier family 22 member 8
SLC47A1 [MATE1]	Hs00217320_m1	solute carrier family 47 member 1
SLC47A2 [MATE2-K]	Hs00945652_m1	solute carrier family 47 member 2
SLCO4C1 [OATP4C1]	Hs00698884_m1	solute carrier organic anion transporter family member 4C1
SLC5A1 [SGLT1]	Hs01573793_m1	solute carrier family 5 member 1
SLC5A2 [SGLT2]	Hs00894642_m1	solute carrier family 5 member 2
GAPDH	Hs99999905_m1	glyceraldehyde-3-phosphate dehydrogenase
TBP	Hs00427620_m1	TATA-box binding protein

Gene expression statistical analysis
Statistically significant differences between -ΔCt values were determined for each sample relative to 2D-plastic using unpaired t-tests corrected for multiple comparisons using the Holm-Sidak method, assuming the same scatter (SD) among samples, with $\alpha = 0.05$. Calculations were performed using GraphPad Prism 8.

Tab. S4: Gene expression statistical analysis

Different samples (n = 3) were analyzed using unpaired t-tests relative to 2D-plastic using -ΔCt values. The table summarizes the adjusted P-value and statistical significance differences (P < 0.05) (Signf.)

Gene	MPS-day 2		MPS-day 7		2D-transwell	
	P value	Signf.	P value	Signf.	P value	Signf.
ABCC4	0.9723	No	0.9431	No	0.7031	No
AQP1	0.7684	No	0.1161	No	0.7377	No
CUBN	0.4514	No	0.1255	No	0.5749	No
GAPDH	0.8481	No	0.8824	No	0.9384	No
GGT1	0.2819	No	0.0469	No	0.4048	No
LRP2	0.6622	No	0.0350	No	0.4052	No
SLC47A1	0.0001	**Yes**	< 0.0001	**Yes**	0.0755	No
ABCB1	0.0212	**Yes**	0.0709	No	0.2360	No
SLC12A3	0.6481	No	0.6679	No	0.9894	No
SLC22A2	0.4093	No	0.6841	No	0.4431	No
SLC47A2	0.0126	**Yes**	0.0002	**Yes**	0.8477	No
SLC5A2	0.7438	No	0.7349	No	0.9144	No
SLCO4C1	0.5744	No	0.5095	No	0.8774	No
HNF4A	0.0235	**Yes**	0.0065	**Yes**	0.0064	**Yes**

Tab. S5: Absolute gene expression (Ct values) of the different samples analyzed (n = 3)

Gene	2D-plastic		2D-transwell		MPS-day 2		MPS-day 7		Kidney cortex	
	Mean	SD	Mean	SD	Mean	SD	Mean	SD	Mean	SD
ABCC4	23.24	0.27	23.78	0.08	24.25	0.26	23.71	0.82	26.80	1.48
AQP1	23.74	0.27	23.43	0.73	24.45	0.41	22.37	0.91	22.98	1.64
CUBN	30.51	0.41	31.26	0.58	30.70	0.23	29.18	0.15	24.07	1.38
GGT1	22.80	0.32	21.90	0.49	22.62	0.57	20.90	0.23	22.97	1.67
LRP2	31.11	2.75	32.19	0.68	31.67	1.20	29.06	1.17	22.59	1.35
SLC47A1	33.30	0.20	31.26	0.38	29.66	1.15	27.17	1.13	23.42	1.23
ABCB1	21.56	0.22	23.06	0.18	25.31	0.11	24.34	0.60	25.19	1.19
SLC12A3	21.41	0.55	21.48	0.49	21.94	0.48	21.44	0.76	22.10	0.80
SLC22A2	25.37	0.67	26.37	0.37	27.37	0.78	26.42	0.47	25.22	1.56
SLC47A2	30.14	1.13	30.46	0.82	28.26	1.06	25.93	0.75	23.66	0.92
SLC5A2	34.79	0.19	28.79	5.08	33.04	2.97	31.12	2.77	24.84	2.36
SLCO4C1	22.16	0.53	22.06	0.85	22.57	0.25	21.91	0.86	25.71	1.28
SLC22A6	-	-	-	-	34.17	0.64	29.26	0.85	22.23	1.03
SLC22A8	-	-	-	-	-	-	-	-	24.85	1.58
HNF4A	31.99	1.03	28.27	0.07	28.85	1.30	27.25	1.01	22.05	0.93
HPRT1	23.97	1.18	24.06	0.72	25.03	0.39	24.53	0.68	26.13	0.94
GAPDH	16.77	1.09	16.95	0.26	18.04	0.66	17.15	0.30	21.46	1.23
TBP	22.27	1.68	25.71	0.93	25.28	0.25	24.94	0.79	27.09	0.50

4 Apparent permeability and trans-epithelial flux calculations

The apparent permeability (P_{app}) of metformin and cidofovir was determined in a conventional 2D-transwell assay, in the apical-to-basolateral (A2B) direction and the basolateral-to-apical (B2A) direction. The efflux ratio (ER) was determined as $P_{app(B2A)}/P_{app(A2B)}$. An ER > 2 indicates that active transport is involved in the drug permeability.

$$P_{app} = \frac{dQ}{dt.A.Ci}$$

P_{app} is defined as the change in concentration (*dQ*) in the recipient compartment (A or B) over time (*dt*), crossing a barrier area (cell grow surface: *A*) relative to the initial concentration (*Ci*) in the donor compartment (A or B). Units: $cm.s^{-1}.10^{-6}$

Tab. S6: Metformin and cidofovir P_{app} values ($cm.s^{-1}.10^{-6}$) obtained from 2D-transwell experiments
Values represent three independent experiments performed in triplicate and are expressed as mean ± standard deviation. Efflux ratio (ER) is defined as B2A / A2B.

Metformin		**Inhibited (Metformin + Imipramine)**	
A2B	14.4 ± 13.3	**A2B**	14.0 ± 6.6
B2A	13.7 ± 16.7	**B2A**	13.7 ± 8.4
ER	0.95	**ER**	0.98
Cidofovir		**Inhibited (Cidofovir + Probenecid)**	
A2B	12.3 ± 16.3	**A2B**	13.8 ± 6.3
B2A	9.0 ± 11.3	**B2A**	6.3 ± 0.9
ER	0.73	**ER**	0.46

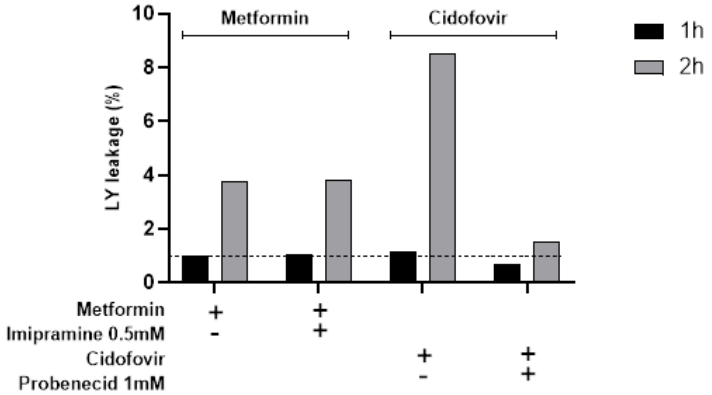

Fig. S3: RPTEC paracellular permeability in the presence of metformin or cidofovir in the presence and absence of inhibitors
Fluorescent tracer lucifer yellow (LY) was used to determine RPTEC paracellular monolayer permeability when cultured in 2D-transwells. The monolayers were considered tight when LY leakage ≤1%. Both in presence of metformin or cidofovir with or without inhibitors, LY leakage is maintained at around 1% after 1 h incubation. At 2 h incubation, LY leakage increases across all treatments, indicating that the RPTEC monolayer loses some integrity. To ensure a tight RPTEC monolayer, metformin and cidofovir permeability assays were performed at 1 h incubation.

Trans-epithelial flux (*J*) calculations were performed to evaluate the movement of drugs from B2A in 2D-transwell and kidney-MPS. This permeability analysis accounts for the quantity of a drug (*m*) crossing the area of a barrier (*A*) to a recipient compartment over time (*t*), independent of the initial concentration in the donor compartment. Units: $\mu mol.cm^{-2}.min^{-1}$.

$$J = \frac{m}{A.t}$$

5 Shear stress calculations in kidney-MPS

To estimate the shear stress experienced by RPTEC in the kidney-MPS chip, an online microfluidic flow rate and shear stress calculator was used (https://darwin-microfluidics.com/blogs/tools/microfluidic-flowrate-and-shear-stress-calculator). The dimensions of the tubule embedded in the MPS chip matrix were used (diameter: 125 µm; length: 5.8 mm), together with a viscosity of 0.7978 cP. Flow rates of either 0.5 µL/min (kidney-MPS culture conditions) or 1 µL/min (kidney-MPS assay conditions) were used to estimate shear stress.

Tab. S7: Shear stress calculation and laminar flow parameters

Flow rate	0.5	1	µL/min
Pressure	0.064	0.129	mbar
Resistance	1.287	1.287	mbar.min/µL
Reynold number	0.106	0.213	-
Wall shear stress	0.347	0.693	dyne/cm^2
Velocity	0.679	1.358	mm/s

6 MPS-chip renal tubule cell count

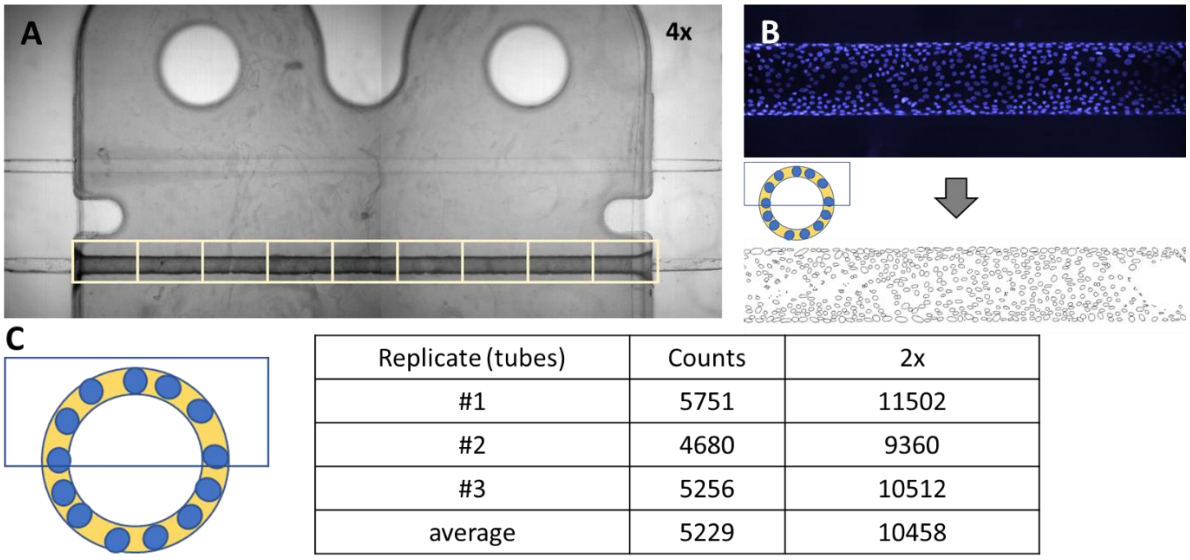

Replicate (tubes)	Counts	2x
#1	5751	11502
#2	4680	9360
#3	5256	10512
average	5229	10458

Fig. S4: Depiction of the cell count workflow in kidney-MPS using ImageJ
Cell density in the renal tubule was estimated by counting the number of nuclei present in renal tubules. The renal tubule was split into 9 sections (A), and confocal stacks of 25 images (20x) from the midsection to the boundary of the tubule were acquired using a CV7000 imager (B-C). In ImageJ image stacks were projected to compile all structures present in one section (B), and the nucleus number was calculated. ImageJ instructions used were as follows:
1. Load image. Image → Type → 8 bit colour
2. Process → Binary → make binary
3. Process → Binary → Watershed
4. Analyse → analyse particles
5. Show: outlines
6. Display results
7. Summarize
8. *In situ* show.
The number of nuclei estimated reflects ½ of a tubule, and assuming a homogenous distribution of cells in the tubules, the values were doubled to estimate the whole renal tubule. Confocal stacks of the whole circumference of the renal tubule were not used since this would skew the total number of cells given that both the nucleus from the bottom and top half of the tubule are super-imposed.

7 Metformin and cidofovir perfusion cytotoxicity

To evaluate any cytotoxic effects in the kidney-MPS after perfusion with metformin or cidofovir, live-dead assays were applied. Assays were performed after a 6-h perfusion with metformin or cidofovir together with the inhibitors imipramine or probenecid, respectively.

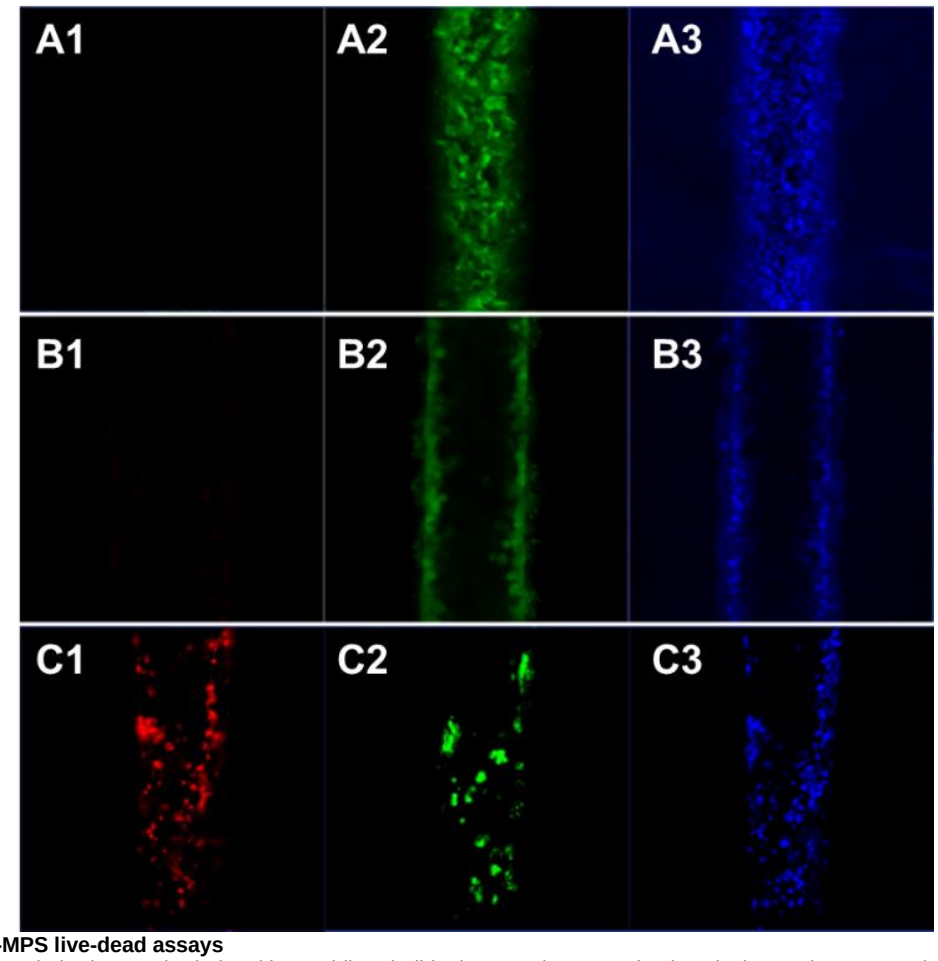

Fig. S5: Kidney-MPS live-dead assays
Chips were perfused via the renal tubule with propidium iodide (PI, 1 µg/mL, panels 1), calcein-AM (1 µM, panels 2) and Hoechst 33342 for 1 h (1:1000, panels 3). Non-viable cells with their membrane integrity compromised incorporate PI (red), viable cells metabolize calcein-AM and retain calcein (green), nuclei are highlighted in blue. Cytotoxicity was not observed in the renal tubules perfused with metformin (A1-3) or cidofovir (B1-3), evident from the lack of PI accumulation. In a renal tubule with compromised viability (C1-3), PI permeates into cells, calcein metabolism is limited and nuclear stain is reduced due to cell loss.

8 Quantification of trans-epithelial drug transport in the micro-perfusion platform

The micro-perfusion model
A semi-mechanistic modelling approach, schematically illustrated in Figure 6A (main text), was developed to evaluate drug disposition in the kidney-MPS chip. The model considers the net diffusion of drug cross the physical extracellular matrix volume section V_{tot} separating the loading and renal microfluidic channels, and further the basolateral-to-apical transport into the renal channel (Tab. S8). V_{tot} is split into n_{tr} well-stirred transit compartments of equal volume $V_{tr} = V_{tot}/n_{tr}$ to accommodate for the transit time through the matrix. The flux of drug at any time t into the first transit compartment is proportional to the concentration $C_l(t)$ in the loading channel, as defined by a first-order rate constant Q_{tr} [µL/min] (Eq. S1). The same rate constant further defines flux into subsequent transit volumes and, in the cell-free chip presenting no epithelial cell barrier to passage, also transport into the renal channel (Eq. S2-S4). Drug is in turn leaving the renal channel at a rate governed by the chip perfusion rate Q_p [µL/min] on its path to the outlet collection port. In the presence of a RPTEC monolayer, drug translocates from the extracellular matrix to the renal channel either by diffusion down its concentration gradient (trans- or paracellularly) or by transporter-mediated secretion, categorized here as 'passive' and 'active' transport, respectively (Eq. S5). We expect the amount of drug transported to depend on the tubular area formed by the RPTECs, and hence define the rate constants as permeability-surface area products, denoted PS_p and PS_a [µL/min] for active and passive transport, respectively. A set of ordinary differential equations following mass-action principles forms a mathematical representation of the above. The rate by which the amount of drug $X_{tr,i}$ changes over time is given by

$$\frac{dX_{tr,1}}{dt} = Q_{tr} \times (C_l(t) - \frac{X_{tr,1}}{V_{tr}}) \qquad \text{Eq. S1}$$

for the first transit compartment i = 1, where $C_l(t)$ represents the concentration in the loading channel. Change in subsequent compartments i = 2:n_{tr}-1 follows

$$\frac{dX_{tr,i}}{dt} = \frac{Q_{tr}}{V_{tr}} \times \left(X_{tr,i-1} - X_{tr,i}\right), \quad \text{Eq. S2}$$

whereas

$$\frac{dX_{tr,n}}{dt} = \frac{1}{V_{tr}} \times \left(Q_{tr} \times X_{tr,n-1} - \max\left(Q_{tr} \middle| PS_a + PS_p\right) \times X_{tr,n}\right) \quad \text{Eq. S3}$$

defines flux into and out of the last transit compartment $i = n_{tr}$. The rate equation follows the assumption that sink conditions apply, with continuous flow though the tubule, and passive reabsorption is negligible. Following the reasoning above, change to the amount in the renal channel X_r is expressed as

$$\frac{dX_r}{dt} = Q_{tr} \times \frac{X_{tr,n}}{V_{tr}} - Q_p \times \frac{X_r}{V_{ch}} \quad \text{Eq. S4}$$

at empty cell-free chip conditions, whereas for the situation with a renal tubule, X_r is governed by

$$\frac{dX_r}{dt} = (PS_a + PS_p) \times \frac{X_{tr,n}}{V_{tr}} - Q_p \times \frac{X_r}{V_{ch}}, \quad \text{Eq. S5}$$

where Q_p, PS_p and PS_a represent the perfusion rate, and active and passive permeability-surface areas, respectively.

Assumptions and modelling steps

In the micro-perfusion model described, kinetic parameters Q_{tr}, PS_p, and PS_a and number of transit compartments n_{tr} are not directly given by experimental conditions (Tab. S8) and need estimation through optimization of a likelihood function of the fit to observed concentrations. Identification required the following general assumptions: i) flux of drug through the loading channel and subsequent dispersion into the extracellular matrix in the presence of a RPTEC monolayer can be approximated in a cell-free chip setup, ii) concentration-time profiles at the outlet ports of each circuit are useful surrogates for profiles in the channels through the matrix chamber, and iii) the loading and renal channels can be considered well-mixed compartments.

Tab. S8: Model parameters defining experimental conditions and chip geometries

Parameter	Symbol	Unit	Value
Perfusion rate	Q_p	µL/min	1.0
Channel diameter	d_{ch}	mm	0.125
Channel length	l_{ch}	mm	5.8
Channel volume	V_{ch}	µL	0.0712
Channel separation		mm	1.0
ECM volume separating the microfluidic channels[a]	V_{tot}	µL	0.725

[a] Product of channel length, diameter, and distance separating the channels.

The loading outlet profile after perfusion of drug through a cell-free chip over 6 hours demonstrates significant overlap to observations from chip with RPTEC tubule ± selective inhibitors (Fig. S6). This suggests that of the continuously introduced drug, the fraction dispersed into the extracellular matrix is relatively insensitive to the experimental condition over this time period, supporting assumption i). For reasons indicated above, including the consequence of flow profile and interactions with material, we expect a broadening of the concentration-time build-up along the length of each microfluidic circuit, also downstream of the matrix chamber. However, as loading and renal profiles are expected to be similarly convoluted, actual channel profiles – provided linear kinetics – will be interchangeable with observed port profiles in assessing exchange across the channels, in support of assumption ii). Finally, given the small volume and short residence time in the matrix loading and renal channels (< 0.1 min at experimental conditions), influence of axial concentration gradients is negligible, in line with assumption iii).

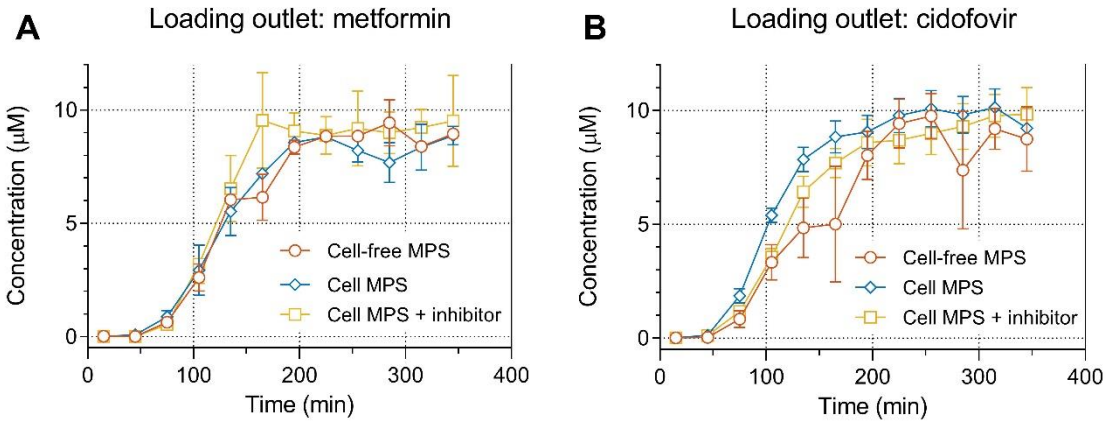

Fig. S6: Loading channel outlet profiles
Comparison of loading channel outlet profiles following perfusion at 10 µM of metformin (A) or cidofovir (B) through cell-free (red circles) or renal tubule chips in the absence (blue diamonds) and presence (yellow squares) of inhibitor over 6 h. Symbols represent the mean values and bars the associated standard error (n = 3).

Parameters defining renal secretion in the MPS system, PS_p and PS_a ultimately used to predict human renal clearance, were estimated for each drug by a sequential fitting procedure. The cell-free chip profiles were used to calibrate the model's baseline behavior. Firstly, the loading channel $C_l(t)$ was modelled empirically by curve-fitting of a sigmoidal three-parameter function to the loading channel outlet concentration.

$$C_l(t) = \frac{Top}{1 + 10^{(\log(t_{50}) - \log(t)) * \gamma}} \qquad \text{Eq. S6}$$

Definition of *Top* (concentration at the plateau), t_{50} (time at which C_l = *Top*/2) and γ (slope factor) allowed for simulation of the concentration driving flux into the extracellular matrix (Eq. S1) at any time *t*. This in turn enabled subsequent estimation of Q_{tr} by fitting the micro-perfusion model to the corresponding renal outlet profile (Fig. 6B1,C1, main text). Keeping $C_l(t)$ and Q_{tr} frozen, basolateral-to-apical transport of the epithelial cell layer, represented by parameters PS_p and PS_a, was assessed by simultaneous fit to renal channel outlets in the absence and presence of selective inhibitors of the carrier-mediated pathway (Fig. 6B2,C2, main text). Parameter estimates for metformin and cidofovir are collected in Table 1 (main text). Estimates were found to be insensitive to number of transit compartments ≥ 3. Reported estimates were obtained for n_{tr} = 3.

Software implementation
The micro-perfusion model was implemented in MATLAB (Release 2017a, The MathWorks, Inc., Natick, MA, US). Fitting applied a naïve pooled approach using the non-linear least squares solver *lsqnonlin* with the default trust-region-reflective algorithm. Model selection was guided by a composite of likelihood function optimization and visual inspection of the residual graphs. Confidence intervals were generated by Monte-Carlo simulations (n = 500) of concentration-time profiles on basis of parameter values randomly chosen from the multivariate normal distribution of the estimates, generated from the *mvnrnd* function, as implemented in MATLAB. At each simulated timepoint, upper and lower bounds were given by the 97.5th and 2.5th percentiles, respectively.

9 *In vitro* to *in vivo* extrapolation (IVIVE)

The renal clearance in human was predicted from PS_p and PS_a on the basis of the tubular surface area in the microfluidic system relative to that of the *in vivo* physiology following the scaling method established by Kunze et al. (2014). In brief, the approach expresses kidney organ clearance $CL_{r,org}$ as the net result of glomerular filtration $CL_{r,fil}$, tubular secretion $CL_{r,sec}$, and fractional tubular reabsorption f_{reab}.

$$CL_{r,org} = (CL_{r,fil} + CL_{r,sec}) \times (1 - f_{reab}) \qquad \text{Eq. S9}$$

Filtration is calculated from the glomerular filtration rate *GFR* and the fraction unbound in blood fu_b

$$CL_{r,fil} = fu_b \times GFR, \qquad \text{Eq. S10}$$

whereas secretion is derived from the renal blood flow rate $Q_{r,b}$, fu_b and the scaled intrinsic clearance of tubular transport $CL_{int,sec}$

$$CL_{r,sec} = \frac{Q_{r,b} \times fu_b \times CL_{int,sec}}{Q_{r,b} + fu_b \times CL_{int,sec}} \quad \text{Eq. S11}$$

applying the well-stirred liver model concept. Reabsorption from the tubule fluid is calculated as

$$f_{reab} = \frac{CL_{int,reab}}{GFR + CL_{int,reab}}, \quad \text{Eq. S12}$$

where the intrinsic clearance of reabsorption *in vivo* $CL_{int,reab}$ constitutes the passive portion of $CL_{int,sec}$. The *in vivo* intrinsic clearances were upscaled from the MPS determined permeability-surfaces areas

$$CL_{int,sec} = (PS_a + PS_p) \times \frac{SA_{vivo}}{SA_{MPS}} \quad \text{Eq. S13}$$

$$CL_{int,reab} = PS_p \times \frac{SA_{vivo}}{SA_{MPS}}, \quad \text{Eq. S14}$$

where SA_{vivo} is the estimated total surface area of a human proximal tubules and SA_{MPS} is the surface area of the RPTEC tubule layer in the microphysiological system:

$$SA_{vivo} = \frac{\pi \times d_{PT} \times l_{PT} \times n_{neph} \times n_{kid}}{BW} \quad \text{Eq. S15}$$

$$SA_{MPS} = \pi \times d_{ch} \times l_{ch} \quad \text{Eq. S16}$$

Physiological values (Tab. S9) for the proximal tubule diameter d_{PT} and length l_{PT}, number of nephrons per kidney n_{neph}, number of kidneys n_{kid}, and body weight *BW* were taken from literature (Lote, 2013) following the steps of Kunze et al. (2014). Sensitivity of metformin and cidofovir predicted renal clearance to variation of *in vitro* (MPS surface area) and physiological (*in vivo* surface area, GFR and renal blood flow) scaling parameters are shown in Figure S7. A 3-fold change of each parameter resulted in predicted renal clearance within a factor of 2 of the point estimate, with the expectation of GFR for which the clearance was within a factor of 3.

Tab. S9: Physiological numbers for estimation of a human proximal tubule surface area SA_{vivo} (adapted from Kunze et al., 2014)

Parameter	Symbol	Unit	Value
PT length	l_{PT}	mm	15.0
PT diameter	d_{PT}	mm	0.070
Number of nephrons/kidneys	n_{neph}	-	1.50E+06
Number of kidneys	n_{kid}	-	2
Glomerular filtration rate	*GFR*	mL/min	120
Renal blood flow	$Q_{r,b}$	mL/min	1.20E+03

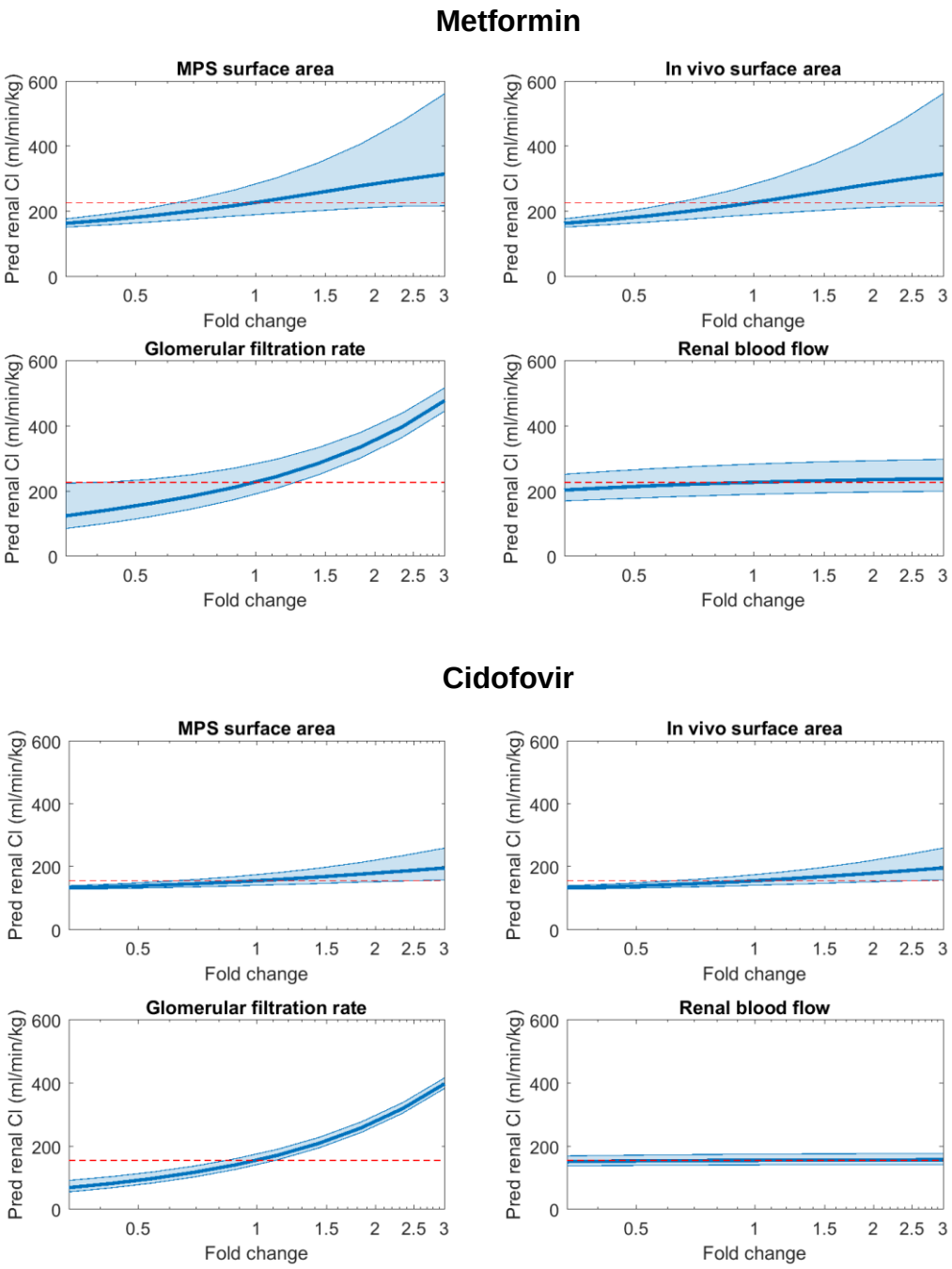

Fig. S7: **Sensitivity analysis**
Sensitivity of metformin (top) and cidofovir (bottom) predicted renal clearance to variation of individual *in vitro* (MPS surface area) and physiological (*in vivo* surface area, GFR and renal blood flow) scaling parameters. Best-fit simulations and 95% confidence range indicated by solid lines and shaded areas, respectively, as each parameter is varied. Red line indicates the point estimate for the renal clearance.

10 The steady-state model

The permeability-surface area products ($PS_{passive}$ and PS_{active}) were derived at steady-state, when drug concentration in the loading channel reaches a constant input, approximately 200 minutes after perfusion is initiated. In Equation S7, *Cd* and *Cr* are approximated by the loading and renal channel outlet concentrations, and *Vr/t* is the flow rate (1 µL/min in this setup). The apparent permeability coefficient (P_{app}) is defined in Equation S8, where *SA* corresponds to the surface area.

$$PS = \frac{Vr \times Cr,ss}{t \times Cd,ss}$$ Eq. S7

$$Papp = \frac{Vr \times Cr}{t \times SA \times Cd}$$ Eq. S8

Tab. S10: Permeability parameters, derived using the steady-state model
The receiver volume (*Vr*) considered for the calculations was 1.00E-3 cm^3 and a surface area (*SA*) of 0.023 cm^2

Parameter	Predictions	
	Metformin	**Cidofovir**
Donor conc. Cd (µM)	9.05	9.6
Receiver conc. Cr (µM)	1.23	0.4
Receiver conc. + inhibitor Cr (µM)	0.13	0.13
P_{app} (cm/min)	0.00599	0.00177
P_{app} + inhibitor (cm/min)	0.00063	0.00060
PS_{active}+ $PS_{passive}$ (µL/min)	0.14	0.040
$P_{passive}$ (µL/min)	0.014	0.014
P_{active} (µL/min)	0.12	0.027

References

Kunze, A., Huwyler, J., Poller, B. et al. (2014). In vitro-in vivo extrapolation method to predict human renal clearance of drugs. *J Pharm Sci 103*, 994-1001. doi:10.1002/jps.23851

Lote, C. J. (ed.) (2013). *Principles of Renal Physiology*. 5th edition. Springer. doi:10.1007/978-1-4614-3785-7

Zou, L., Stecula, A., Gupta, A. et al. (2018). Molecular mechanisms for species differences in organic anion transporter 1, OAT1: Implications for renal drug toxicity. *Mol Pharmacol 94*, 689-699. doi:10.1124/mol.117.111153